TLR-activated mesenchymal stromal cell therapy and antibiotics to treat multi-drug resistant *Staphylococcal* septic arthritis in an equine model

Lynn M. Pezzanite[1]^, Lyndah Chow[1]^, Jennifer Phillips[1], Gregg M. Griffenhagen[1]^, A. Russell Moore[2]^, Thomas P. Schaer[3], Julie B. Engiles[3,4]^, Natasha Werpy[5], Jessica Gilbertie[6]^, Lauren V. Schnabel[7]^, Doug Antczak[8], Donald Miller[8]^, Steven Dow[1,2]^, Laurie R. Goodrich[1]^

[1]Department of Clinical Sciences, College of Veterinary Medicine and Biomedical Sciences, Colorado State University, Fort Collins, CO, USA; [2]Department of Microbiology, Immunology and Pathology, College of Veterinary Medicine and Biomedical Sciences, Colorado State University, Fort Collins, CO, USA; [3]Department of Clinical Studies, New Bolton Center, School of Veterinary Medicine, University of Pennsylvania, Kennett Square, PA, USA; [4]Department of Pathobiology, New Bolton Center, School of Veterinary Medicine, University of Pennsylvania, Kennett Square, PA, USA; [5]Ocala Equine Hospital, Ocala, FL, USA; [6]Department of Microbiology and Immunology, Edward Via College of Osteopathic Medicine, Blacksburg, VA, USA; [7]Department of Clinical Sciences, College of Veterinary Medicine and Biomedical Sciences, North Carolina State University, Raleigh, NC, USA; [8]Baker Institute, College of Veterinary Medicine, Cornell University, Ithaca, NY, USA

Contributions: (I) Conception and design: LM Pezzanite, L Chow, GM Griffenhagen, TP Schaer, JB Engiles, J Gilbertie, LV Schnabel, D Antczak, D Miller, S Dow, LR Goodrich; (II) Administrative support: LM Pezzanite, L Chow, AR Moore, TP Schaer, JB Engiles, J Gilbertie, LV Schnabel, S Dow, LR Goodrich; (III) Provision of study materials or patients: LM Pezzanite, L Chow, GM Griffenhagen, S Dow, LR Goodrich; (IV) Collection and assembly of data: LM Pezzanite, L Chow, GM Griffenhagen, D Antczak, D Miller, AR Moore, JB Engiles, N Werpy, LR Goodrich; (V) Data analysis and interpretation: LM Pezzanite, L Chow, GM Griffenhagen, D Antczak, D Miller, AR Moore, TP Schaer, JB Engiles, N Werpy, S Dow, LR Goodrich; (VI) Manuscript writing: All authors; (VII) Final approval of manuscript: All authors.

Correspondence to: Laurie R. Goodrich, DVM, MS, PhD. Orthopaedic Research Center, C. Wayne McIlwraith Translational Medicine Institute, Department of Clinical Sciences, College of Veterinary Medicine, Colorado State University, Fort Collins, CO, USA.
Email: Laurie.goodrich@colostate.edu.

Background: Rapid development of antibiotic resistance necessitates advancement of novel therapeutic strategies to treat infection. Mesenchymal stromal cells (MSC) possess antimicrobial and immunomodulatory properties, mediated through antimicrobial peptide secretion and recruitment of innate immune cells including neutrophils and monocytes. TLR-3 activation of human, canine and equine MSC has been shown to enhance bacterial killing and clearance *in vitro*, in rodent *Staphylococcal* biofilm infection models and dogs with spontaneous multi-drug-resistant infections. The objective of this study was to determine if intra-articular (IA) TLR-3-activated MSC with antibiotics improved clinical parameters and reduced bacterial counts and inflammatory cytokine concentrations in synovial fluid (SF) of horses with induced septic arthritis.

Methods: Eight horses were inoculated in one tarsocrural joint with multidrug-resistant *Staphylococcus aureus* (*S. aureus*). Bone marrow-derived MSC from three unrelated donors were activated with TLR-3 agonist polyinosinic, polycytidylic acid (pIC). Recipient horses received MSC plus vancomycin (TLR-MSC-VAN), or vancomycin (VAN) alone, on days 1, 4, 7 post-inoculation and systemic gentamicin. Pain scores, quantitative bacterial counts (SF, synovium), SF analyses, complete blood counts, cytokine concentrations (SF, plasma), imaging changes (MRI, ultrasound, radiographs), macroscopic joint scores and histologic changes

^ ORCID: Lynn M. Pezzanite, 0000-0003-4990-5006; Lyndah Chow, 0000-0002-6413-9517; Gregg M. Griffenhagen, 0000-0003-3522-5587; A. Russell Moore, 0000-0003-4904-8788; Julie B. Engiles, 0000-0001-9057-2093; Jessica Gilbertie, 0000-0002-4953-6717; Lauren V. Schnabel, 0000-0002-1993-8141; Donald Miller, 0000-0002-4868-1007; Steven Dow, 0000-0001-5488-9464; Laurie R. Goodrich, 0000-0002-8010-4429.

were assessed. Results were reported as mean ± SEM.

Results: Pain scores (d7, P=0.01, 15.2±0.2 *vs.* 17.9±0.5), ultrasound (d7, P=0.03, 9.0±0.6 *vs.* 11.8±0.5), quantitative bacterial counts (SF d7, P=0.02, 0±0 *vs.* 3.4±0.4; synovium P=0.003, 0.4±0.4 *vs.* 162.7±18.4), systemic neutrophil (d4, P=0.03, 4.6±0.6 *vs.* 7.8±0.6) and serum amyloid A (SAA) (d4, P=0.01, 1,106.0±659.0 *vs.* 2,858.8±141.3; d7, P=0.02, 761.8±746.2 *vs.* 2,357.3±304.3), and SF lactate (d7, P<0.0001, 5.4±0.2 *vs.* 15.0±0.3), SAA (endterm, P=0.01, 0.0 *vs.* 2,094.0±601.6), IL-6 (P=0.03, 313.0±119.2 *vs.* 1,328.2±208.9), and IL-18 (P=0.02, 11.1±0.5 *vs.* 13.3±3.8) were improved in TLR-MSC-VAN *vs.* VAN horses. Study limitations include the small horse sample size, short study duration, and lack of additional control groups.

Conclusions: Combined TLR-activated MSC with antibiotic therapy may be a promising approach to manage joint infections with drug resistant bacteria.

Keywords: Antibiotic resistance; infectious arthritis; mesenchymal stromal cell (MSC)

Submitted Apr 02, 2022. Accepted for publication Sep 23, 2022.
doi: 10.21037/atm-22-1746
View this article at: https://dx.doi.org/10.21037/atm-22-1746

Introduction

Development of antibiotic resistance necessitates advancement of novel therapeutic strategies to treat infection. Regenerative therapies such as mesenchymal stromal cells (MSC) are appealing as they have inherent antimicrobial, anti-inflammatory, and immunomodulatory properties, which can be augmented by immune activation and play a role in resolution of inflammation associated with infection (1-7). MSC produce chemokines such as MCP-1 and IL-8 that stimulate recruitment and activation of monocytes and neutrophils, respectively, and also secrete antimicrobial peptides (AMPs), which are directly bactericidal (2,8-18). Previous studies have demonstrated that the antimicrobial and immunomodulatory properties of MSC, including AMP secretion, direct inhibition of bacterial growth, secretion of immunomodulatory cytokines, and neutrophil phagocytosis of bacteria, can be enhanced by stimulation with TLR ligands *in vitro* (TLR-3, TLR-4 and TLR-9) (2,10,18). In a chronic implant infection model in mice, MSC activated with TLR-3 ligand polyinosinic:polycytidylic acid (pIC) demonstrated synergism with antibiotics to eliminate chronic *Staphylococcus aureus* (*S. aureus*) infection, with improved activity compared to non-activated MSC with or without antibiotics, or antibiotics alone (18). The findings from the mouse model were also confirmed in a clinical study in dogs with spontaneous drug-resistant infections treated systemically with activated MSC and antibiotics (18).

These initial studies prompted us to evaluate the potential utility of cell-based therapies in a translational large animal (equine) model of drug-resistant joint infection. The investigation of novel cellular therapies in large animal disease models is critical to assessing and validating safety and efficacy of treatments for human orthopedic infections (18). The equine preclinical model of septic arthritis is a clinically relevant translational model for human joint infections, with greater similarity in joint volume, cartilage thickness and articular cartilage loading forces to that of humans than small animal laboratory species (19-25). In addition, the large joint volume of horses allows for repeated collection of synovial fluid (SF) for analyses, greatly enhancing the scientific robustness while decreasing the number of animals required when compared to lower vertebrate models (19-22,24,25). Development of septic arthritis is a naturally occurring disease process in horses and is well-documented (26-30). Bacterial biofilm aggregate formation in equine SF has recently been described, providing further evidence of relevance for the equine model of septic arthritis for human disease (25). Equine MSC generate bactericidal activity against both Gram-negative and positive bacteria, mediated through secretion of four AMPs (4), and this bactericidal activity can be upregulated by TLR-3 MSC activation (10).

Therefore, we conducted studies to evaluate whether TLR-3 activated bone-marrow-derived allogeneic MSC combined with antibiotics administered IA would improve lameness and reduce inflammatory biomarkers and bacterial burden an equine model of septic arthritis, *vs.* antibiotics alone. We hypothesized that combination therapy would result in more rapid resolution of bacterial infection and

synovial markers of inflammation compared to antibiotic treatment alone. Key findings were that treatment with immune activated equine MSC therapy plus vancomycin (VAN) significantly reduced bacterial concentrations in both the SF and the synovium and decreased pro-inflammatory cytokine concentrations in SF compared to VAN therapy alone. Overall, lameness as a function of pain was markedly decreased in treated animals. Repeated injections of activated MSC injection were well-tolerated clinically and led to rapid improvement in clinical scores, suggesting a similar treatment approach may be warranted for treatment of drug resistant infectious arthritis in human patients. We present the following article in accordance with the ARRIVE reporting checklist (available at https://atm.amegroups.com/article/view/10.21037/atm-22-1746/rc).

Methods

Study design

The Institutional Animal Care and Use Committee at Colorado State University (No. CSU IACUC #977) approved this study. All methods were conducted according to the national guidelines under which the institution operates, and NIH Guidelines for the Care and Use of Laboratory Animals (8th edition). Horses (n=8 total) were randomized by leg to receive either treatment TLR-activated MSC and vancomycin (TLR-MSC-VAN) or control VAN alone by random number generator (random.org). Sample size (n=4 horses/group) was based on previous literature (31), and following pilot studies in horses with the septic arthritis model with pain scoring as the primary outcome measure. Analyses included all horses for all parameters evaluated. One co-author (LP) performed treatment allocation randomization of experimental unit (i.e., individual horses) while other co-investigators were blinded to treatment throughout the course of the study.

Horses were enrolled in four cohorts (two/cohort) (*Figure 1*). On day 0, intravenous jugular catheters were placed, and horses were inoculated intra-articularly in one randomly assigned tibiotarsal joint with 1×10^4 colony forming units (CFU) *S. aureus* [methicillin resistant *S. aureus* (MRSA) strain USA300] bacteria, as previously described (32). Horses then were treated on d1, 4, and 7 with either 20×10^6 pooled bone-marrow-derived allogeneic MSC and VAN (TLR-MSC-VAN) or VAN alone, with cell dose based on a previous report (33). Horses were administered systemic antibiotics [gentamicin 6.6 mg/kg intravenously (IV) q24h] which was selected based on culture and sensitivity results to the proposed bacterial isolate beginning 24 h following inoculation until end-term (d7) for VAN or d10 for TLR-MSC-VAN. Horses were euthanized on d7 (VAN) or d14 (TLR-MSC-VAN). VAN-treated horses were humanely euthanized at the earlier time point due to observed increased pain and inflammation scores during pilot studies.

For IA inoculation and treatment, horses were sedated with detomidine (0.01–0.02 mg/kg IV) and butorphanol tartrate (0.01 mg/kg IV) to effect. Tibiotarsal joints were aseptically prepared with chlorhexidine gluconate (4%, VetOne, MWI, Boise, ID, 83705) followed by 70% ethanol. VAN dose (100 mg) was determined in a pilot study based on assessment of antibiotic levels in SF by immunoassay over 72 h following VAN (100 mg) injection in the tarsocrural joint of one normal horse, in combination with *in vitro* studies to determine cytotoxicity of VAN to equine MSC (Figure S1).

For pain management, all horses received epidural analgesia (Cd2-Cd3) consisting of detomidine (6 mg) and morphine (30 mg) with 20 mL saline at inoculation. Additional epidurals were performed in control horses on d5,6 if deemed necessary based on pain scoring and clinical assessment. Horses were maintained on nonsteroidal anti-inflammatories [(phenylbutazone 200 mg/mL, VetOne, MWI, Boise, ID 83705) 2.2 mg/kg IV q12h] for study duration, with first dose administered at inoculation. Pain/lameness scoring were assessed daily by a veterinarian blinded to study design.

Animals

Use of eight healthy 3–4-year-old horses (3 stallions, 3 geldings, 2 mares) as study subjects was approved by CSU IACUC (protocol #977). Horses were determined to be systemically healthy by physical examination, complete blood count, free of *Salmonella spp.* by fecal polymerase chain reaction (PCR), lameness evaluation performed by two observers board-certified in veterinary surgery (LG, LP) and bilateral radiographs of the tarsi (four-view per limb). Horses were required to be sound in the hindlimbs at the trot and free of radiographic evidence of tarsal osteoarthritis prior to study enrollment. Horses were quarantined for >14 d or until meeting above criteria for enrollment and acclimated to stalls for 5 to 7 d prior to inoculation.

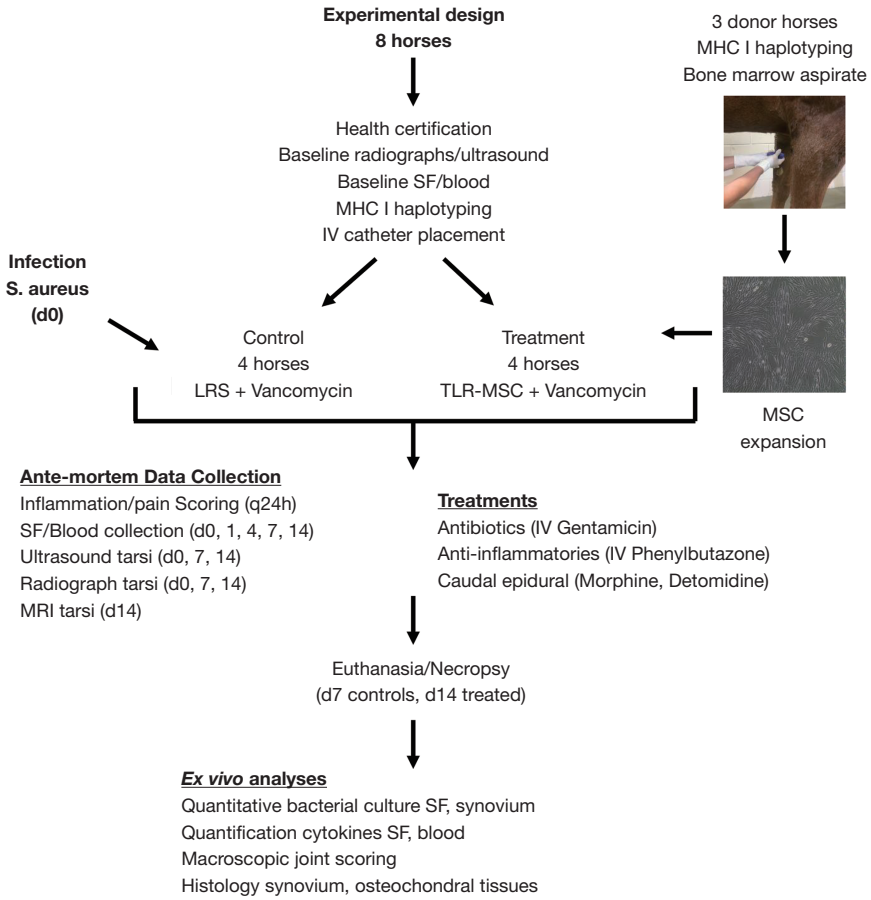

Figure 1 Schematic overview of the study design for the in vivo model of infectious arthritis in horses. Horses (n=8) were quarantined 14 days and acclimated to stalls for 5 to 7 days in cohorts of 2 prior to the beginning of each cohort. Horses were determined to be systemically healthy based on physical examination, lameness evaluation, negative salmonellosis testing, and normal complete blood count before study enrollment. MHC haplotypes were determined. On day 0 of each cohort, each horse was inoculated in one randomly assigned tarsocrural joint with S. aureus. On day 1, 4, and 7 horses were treated intra-articularly with VAN and LRS or VAN and TLR-3 activated MSC (TLR-MSC-VAN). All horses received Cd2-Cd3 epidurals with morphine (30 mg) and detomidine (6 mg) on day 0, systemic antibiotics [gentamicin 6.6 mg/kg IV every 24 hours until d7 (end-term) for VAN, d10 for TLR-MSC-VAN] and nonsteroidal-anti-inflammatories (phenylbutazone 2.2 mg/kg IV every 12 hours until euthanasia). Pain and inflammation scoring were performed daily. SF and blood samples were obtained on days 0, 1, 4, 7 and 14. Radiographic and ultrasonographic evaluations were performed at baseline and days 7 and 14. MRI was performed at end-term (d7 for controls and d14 for treated horses). *Ex vivo* analyses consisting of macroscopic scoring of joint tissues, histopathology, biomarker analysis, bacterial identification and quantitative bacterial counts on synovial fluid and synovium were performed. MHC, major histocompatibility complex; SF, synovial fluid; IV, intravenously; LRS, lactated ringer's solution; MSC, mesenchymal stromal cells; VAN, vancomycin.

Three different 3-year-old Quarter Horses (1 mare, 2 geldings) determined to be healthy by physical examination and bloodwork (complete blood count, serum biochemistry) served as bone marrow aspirate donors for MSC culture and expansion (CSU IACUC protocol #1101). Conditioned media from MSC was screened for antimicrobial and immunomodulatory activity *in vitro* prior to *in vivo* application (10). All horses were maintained in stalls for the duration of the study with twice daily enrichment by grooming.

Major histocompatibility complex (MHC) haplotype analysis

The MHC haplotype of each MSC donor and recipient horse was determined. DNA was extracted from whole blood using a commercially available kit (Qiagen, Valencia, CA 91355) as previously described (34). DNA fragments were submitted to the Equine Genetics Center at the Baker Institute for Animal Health at Cornell University, and equine leukocyte antigen (ELA) MHC haplotypes were determined as previously described (34). GeneMarker software (SoftGenetics, State College, Pennsylvania) was used to analyze fragment analysis files. Haplotypes were reported when matched to previously characterized haplotypes, and unknown haplotypes were stated when identical haplotypes had not been previously reported (Table S1).

Bacterial culture

The MRSA strain USA300 MRSA derived from a human patient was provided to this group of collaborators by H. Schweizer (CSU) with bacterial culture and sensitivity previously reported elsewhere (10). Bacteria were initially grown in Luria Bertani (LB) broth then frozen at –80 ℃ in 20% glycerol until further use. Bacterial cultures were then grown overnight in antibiotic-free MSC growth medium [Dulbecco's Modified Eagle's Medium (DMEM), 1,000 mg/L glucose, 10% fetal bovine serum (FBS)] the day before inoculation. Bacterial sub-cultures were grown to log phase on the day of intra-articular inoculation in antibiotic-free MSC medium (OD600 of 0.6, corresponding to 7.5 $\log_{10}$ CFU/mL), counted, resuspended in 1 mL phosphate buffered saline (PBS), then maintained on ice for transport and injected immediately. Bacterial inoculum [1×10^4 synovial fluid (CFU)] was calculated based on the optical density and previously determined growth curve equation. Pressure bandages were placed over the injection site for approximately one hour following injection to minimize extravasation of bacterial inoculum into periarticular tissues.

MSC culture

For bone marrow aspirate, donor horses were sedated with detomidine (0.01–0.02 mg/kg IV) and butorphanol tartrate (0.01 mg/kg IV) to effect. The sternum was clipped and aseptically prepared with chlorhexidine gluconate followed by 70% ethanol. Bone marrow aspirate (5 mL) was drawn from a single site between the 4th–6th sternebrae using an 11-gauge Jamshidi needle into a sterile syringe containing 1 mL heparin (1×10^4 U). Bone marrow aspirates were purified via ficoll density gradient centrifugation as previously described (35,36), plated and expanded in culture (37 ℃, 5% CO_2, 95% humidity) to 80% confluence for approximately 10 days in complete growth medium [DMEM with 1,000 mg/L glucose, 10% FBS, penicillin (100 U/mL), streptomycin (100 µg/mL), 1M hydroxyethyl piperazineethanesulfonic acid (HEPES)]. Cells were detached from flasks by trypsinization, then frozen at 5×10^6 cells/mL in freeze media [90% FBS, 10% dimethyl sulfoxide (DMSO)] in liquid nitrogen vapor phase until further use.

Cells from 3 donor horses were thawed quickly in a 37 ℃ water bath and recovered in complete growth medium 72 h under standard incubation conditions (37 ℃, 5% CO_2, 95% humidity) prior to each cell injection, which occurred on d1, 4, 7 following inoculation. MSC were trypsinized and counted using an automated cell counter (Cellometer Auto T4; Nexcelom Bioscience) to obtain 20×10^6 MSC pooled from 3 donors. MSC were stimulated with TLR-3 agonist polyinosinic, pIC at 10 µg/mL (InVivoGen, San Diego, CA, USA) for 2 hours suspended in complete growth media at a concentration of 2×10^6 MSC/mL and incubated at 37 ℃, 5% CO_2, 95% humidity. Activation with TLR-3 agonist pIC was performed based on previous *in vitro* and *in vivo* studies demonstrating enhanced antibacterial and immunomodulatory activity with pIC agonism (10,11,18). MSC were used between passage 1 to 5 for all injections. All MSC used for *in vivo* studies were routinely evaluated for surface phenotype, and found to be $CD44^+CD90^+$, and $CD34^-CD45^-$, using equine cross-reactive antibodies as previously described (37), and in agreement with International Society for Cellular Therapy (ISCT) minimal criteria to define MSC (38).

Determination of VAN concentrations and duration in SF

VAN dose was determined in an initial pilot investigation evaluating toxicity to MSC and duration of time above bacterial isolate minimum inhibitory concentration (MIC) (1 µg/mL). Cell viability (mean ± SD) of bone marrow-derived MSC from 3 donor horses, each in triplicate, was determined after 24 h VAN exposure using trypan blue dye exclusion. Dose response for each concentration was normalized to control, and the data transformed to 'normalized dose response *vs.* $\log_{10}$(concentration)' at which

point the half maximal inhibitory concentration 50 (IC50) was determined by nonlinear regression performed in GraphPad Prism8 (GraphPad Software Inc., La Jolla, CA, USA) (39). Duration of time that VAN remained > MIC for the bacterial isolate used was assessed by injecting 100 mg VAN in the tibiotarsal joint of an additional single pilot horse (3-year-old Quarter Horse mare). Synoviocenteses were performed at times 0, 1, 4, 8, 24, 48, 72 h and VAN concentrations determined using competitive ELISA (BioVision, Milpitas, CA, USA 95035). VAN concentrations were measured in SF of TLR-MSC-VAN or VAN treated horses on d0, 1, 4, 7, 14 by ELISA.

Clinical observations

Horses were evaluated two times per day by observers (board-certified veterinary surgeon and anesthesiologist) blinded to treatment assignments prior to administration of pain medications or collection of other measurements to reduce potential confounding. Animals were evaluated for physical examination parameters, signs of infection including pain on joint palpation, swelling, heat, or lameness. Photographs and videos were recorded daily in the morning prior to nonsteroidal anti-inflammatory administration for blinded grading of lameness, periarticular swelling, and distal limb edema. Thermography images of the injected tibiotarsal joint and contralateral control joint were recorded and relative heat signatures determined subjectively. Joint circumference of the tibiotarsal joint was measured daily using a flexible tape measure. To standardize joint circumference, each joint was marked at the level it was measured for consistency. Pain scores were determined by a board-certified surgeon and anesthesiologist, blinded to treatment, based on five parameters (physical examination, lameness evaluation, distal limb edema, synovial swelling, synovial heat), graded 0 to 3 (0 normal, 3 marked), for a maximum total score of 15.

SF collection

SF (4 mL) was obtained from the injected tibiotarsal joint at d0, 1, 4, 7, and 14 (for treated horses) following infection using a sterile 18-gauge needle and extension set. SF was divided for either immediate fluid analysis, serum amyloid A (SAA), and lactate in EDTA heparinized tubes, or aliquoted and stored at –80 ℃ in Eppendorf tubes pending determination of cytokines via multiplex and ELISA assay.

Clinicopathological parameters

SF samples were evaluated by a board-certified clinical pathologist for fluid analysis including total nucleated cell count (Hematrue, Heska Corp, Loveland CO, USA), refractometric total protein, Wright-Giemsa stained (Aerospray, Logan, UT, USA) direct smears to perform manual leukocyte differential, subjective glycosaminoglycan grading (adequate or disrupted) and subjective erythrocyte quantification (excessive or within normal limits). Blood samples were submitted in EDTA containing tubes for heat precipitation fibrinogen, refractometric total protein, complete blood count (Advia 120; Siemens AG, Munich, Germany) and manual leukocyte differential. Whole blood samples obtained in EDTA containing tubes were centrifuged at 3,000 rpm for 10 minutes, after which plasma was aliquoted and frozen at –80 ℃ until cytokine quantification. SF lactate concentrations were determined by handheld lactate meter (Lactate Plus Portable Lactate Reader, Nova Biomedical, Maltham, MA 02454). SF glucose concentrations were assessed by handheld glucometer (AlphaTrak 2 Blood Glucose Monitoring System, Zoetis, Lincoln, NE 68521).

Euthanasia and necropsy

At study end-term (d7 VAN or d14 TLR-MSC-VAN), horses were euthanized using pentobarbital (1 mL/5 kg body weight) administered via indwelling catheter. The hindlimbs were removed and MRI of both tarsi was performed. The hindlimbs were aseptically prepared and SF samples collected. Tibiotarsal joints were dissected aseptically and photographed for macroscopic morphology. Assessment of macroscopic observations was performed based on photographs of injected and contralateral limbs by two board-certified equine surgeons blinded to treatment. Four parameters (synovial proliferation, subcutaneous thickening/edema, vascularity, and cartilage erosion) were consensus graded 0 to 4 (0= normal, 1= slight abnormalities, 2= mild, 3= moderate, 4= severe) for maximal total score of 16. Synovial membrane samples were obtained from four sites within the joint (dorsomedial, dorsolateral, plantaromedial, and plantarolateral). Four osteochondral samples were taken from the lateral and medial aspects of the trochlea from the dorsal and plantar talus.

Determination of SF cytokine and SAA concentrations

Fluorescent bead-based multiplex assay (Milliplex MAP Equine Cytokine/Chemokine Magnetic Beads Multiplex Assay, Millipore Sigma, Burlington, MA, 01803) was used to quantitatively determine levels of 23 analytes (IL-1α, IL-1β, IL-2, IL-4, IL-5, IL-6, IL-8/CXCL8, IL-10, IL-12, IL-13, IL-17a, IL-18, IP-10, MCP-1, RANTES/CCL5, TNF-α, Eotaxin/CCL11, FGF-2, fractalkine/CS3CL1, G-CSF, GM-CSF, GRO, IFN) in SF and plasma from all time points (d0, 1, 4, 7, 14). Quantification of SAA in SF and plasma was performed using SAA assay kit (StableLab, Epona Biotech Limited, Sligo, Ireland).

Quantitative and qualitative bacterial cultures

Samples of end-term SF and synovium were submitted in blood culture vials to the CSU Diagnostic Pathology Laboratory for bacterial identification and sensitivity pattern (BDTM BactecTM Media, Fisher Scientific, Waltham, MA, 02451). Qualitative bacterial sensitivity patterns were compared to that obtained initially for the injected bacteria. Quantitative bacterial cultures were performed of SF at d0, 1, 4, 7, 14 and of synovium at end-term as previously described (25,32,40). Briefly, to generate quantitative cultures, SF aliquots (250 µL) were centrifuged at 8,000 g for five minutes and supernatant was discarded. The remaining bacterial pellet was then washed three times with PBS, resuspended in 1 mL PBS and incubated shaking with 0.05 mg/mL hyaluronidase at 120 rpm at 37 ℃ to disperse any aggregated bacteria. Samples were then centrifuged again at 8,000 g for 5 minutes and reconstituted in PBS for serial dilution. Synovium obtained aseptically at end-term was weighed and incubated with 1.5 mg/mL type 2 collagenase and 0.05 mg/mL hyaluronidase for one hour then pushed through a tissue strainer. Bacterial load was determined using serial dilutions in PBS and plate counting of CFU and reported as CFU per mL of SF or per gram of synovial tissue.

Diagnostic imaging

All imaging findings were recorded for evaluation by a board-certified veterinary radiologist who was blinded to treatment groups. Ultrasound images of the injected and contralateral tarsi were obtained at days 0, 7, 14 (TLR-MSC-VAN). Images were scored for degree of distention, degree of synovial thickening, degree of fibrinous loculation, and degree of vascularity visualized with power Doppler on a scale of 0 to 3 (0= normal, 1= mild, 2= moderate, 3= markedly abnormal). Character of synovial effusion and presence of hyperechoic foci were scored on a scale of 0 or 1 (0= absent/anechoic, 1= present/echogenic).

Radiographic images of the injected and contralateral tarsi (four-view) were obtained at days 0, 7, and 14 (treated horses). Radiographs were evaluated for osteoarthritis on a scale of 0 to 4 (0= normal, 4= severe change) for osteophyte formation, boney proliferation at the joint capsule attachment, subchondral bone lysis and subchondral bone sclerosis.

MRI of the injected and contralateral tarsi was performed immediately postmortem at end-term. MRI images were graded by a board-certified radiologist blinded to treatment assignments. Evaluation included degree of synovial distension, degree of synovial thickening, degree of fibrinous loculation graded 0 to 3; boney proliferation of joint capsule, subchondral bone lysis, subchondral bone sclerosis, osteophyte formation graded 0 to 4; bone fluid graded 0 to 4; and vascular pattern graded 0 to 4.

Histologic evaluation of osteochondral and synovial tissues

Osteochondral and synovial tissues were collected at end-term from four sites per joint from injected and contralateral joints and fixed in neutral-buffered 10% formalin and zinc fixative. Samples were processed for histologic examination with hematoxylin and eosin staining to assess for inflammatory changes. Samples were formalin fixed 48 h then decalcified in formic acid for 2 to 4 weeks, with solution changes every 3 d. Assessment of histology specimens were scored according to Osteoarthritis Research Society International (OARSI) and modified OARSI histology initiative for osteoarthritis in horses developed for septic arthritis (32,41).

Slides were graded by a board-certified veterinary pathologist who was unaware of treatment assignment. Parameters assessed for synovial sections for the OARSI scoring system were cellular infiltrate, intimal hyperplasia; vascularity, subintimal edema and fibrosis/granulation tissue. Parameters assessed for synovial sections for the modified OARSI scoring system included those above as well as fibrin exudate, cellular infiltrate (neutrophils *vs.* peripheral blood mononuclear cells), and intimal ulceration. Osteochondral sections were assessed for cartilage parameters (chondrocyte necrosis, chondrones, fibrillation/

fissures, focal cell loss, Safranin O stain uptake) and bone parameters (osteochondral lesions, subchondral bone remodeling, subchondral bone activation and osteochondral splitting) (Tables S2,S3).

Statistical analysis

Normality was assessed via Shapiro-Wilk tests as well as distribution of diagnostic plots. The effect of treatment and time were evaluated using two-way analysis of variance with Tukey's adjustment for multiple comparisons test to compare inflammation and pain scores, cytokine concentrations in SF and plasma, quantitative bacterial cultures of SF over time, and systemic clinicopathological parameters and biomarkers of inflammation between treated and control horses. Unpaired *t*-tests were used to compare quantitative bacterial counts in synovium at end-term, total macroscopic scores, and histologic scores. MRI scores at end term and ultrasound scores overall were compared via Kruskall-Wallace tests, and ultrasound scores were compared within groups over time and between groups at each time point using Dunn's test with the Holm correction for multiple comparisons (R package rstatix) (42). Analyses were performed using GraphPad Prism v8.4.1 and R version 4.1.2 ("Bird Hippie") (43), with significance assessed at $P<0.05$. Results are reported as mean±standard error of the mean or median (range) when appropriate within the text.

Results

Elucidation of VAN dosing parameters for intra-articular administration

To determine optimal IA VAN dose, balancing toxicity to MSC with antimicrobial efficacy, VAN toxicity to MSC was assessed *in vitro*, and pilot studies were conducted in healthy horses to elucidate PK parameters. IC50, or concentration of VAN at which 50% MSC cell death occurred, was determined to be 3.658 mg/mL (Figure S1A).

At all-time points tested, SF VAN concentrations remained > MIC (1 µg/mL) for bacterial isolate inoculated when 100 mg was injected (Figure S1B,S1C). Based on these studies, a dose of 100 mg for IA injection was selected. VAN concentrations in SF of TLR-MSC-VAN and VAN treated horses remained > MIC at each time point (days 4, 7, 14) VAN concentrations were variable, which may be attributed to differences in effusion, but were not significantly different between TLR-MSC-VAN and VAN (Figure S1D,S1E).

Impact of combination therapy with activated MSC and VAN on clinical parameters in horses with experimental MRSA septic arthritis

One of the primary endpoints of this study was to assess the impact of activated cellular therapy on clinical signs of septic arthritis, as this is a key milestone for success of a new intervention such as activated allogeneic MSC. We found that TLR-MSC-VAN treatment led to significant reduction in clinical pain scores compared to VAN treated horses (d7 15.2±0.2 *vs.* 17.9±0.5, P=0.01) (*Figure 2*). Lameness was reduced, joint circumference normalized more rapidly, and fevers were noted less frequently in TLR-MSC-VAN treated horses. Complete blood counts revealed lower peripheral neutrophil counts at d4 (4.6±0.6 *vs.* 7.8±0.6, P=0.03) and SAA concentrations at both d4 (1,106.0±659.0 *vs.* 2,858.8±141.3, P=0.01) and d7 (761.8±746.2 *vs.* 2,357.3±304.3, P=0.02) in TLR-MSC-VAN *vs.* VAN horses, respectively (*Figure 3*). No statistically significant differences were seen in the 23 inflammatory analytes assessed in plasma via multiplex assay.

Ultrasound scores were improved in TLR-MSC-VAN *vs.* VAN horses on d7 (9.0±0.6 *vs.* 11.8±0.5, P=0.02) (*Figure 4*). MRI scores were lower (i.e., less severely abnormal) but did not reach statistically significant differences in TLR-MSC-VAN *vs.* VAN horses (8.25±0.5 *vs.* 10.75±1.9, P=0.08), when normalized to contralateral limb scores (*Figure 4*). No statistical differences were detected in conventional radiographic scores between the two treatment groups at any time point with this study. Taken together, these findings indicated that IA administration of activated allogeneic MSC significantly improved clinical signs and imaging correlates associated with septic arthritis.

Response of synovial bacterial counts to treatment with activated MSC

Bacterial counts in SF began to significantly decline in TLR-MSC-VAN treated horses beginning d4 following inoculation, compared to VAN treated animals (*Figure 5*; SF d4, 0.3±0.3 *vs.* 4.2±0.5, P=0.03, d7, 0±0 *vs.* 3.4±0.4, P=0.02; synovium d7, 0.4±0.4 *vs.* 162.7±18.4, P=0.003). This difference became more pronounced as the study progressed, with a 69% reduction at d4 in TLR-MSC-VAN, compared to a 42% increase in VAN animals compared to d1 bacterial counts post inoculation. By d7,

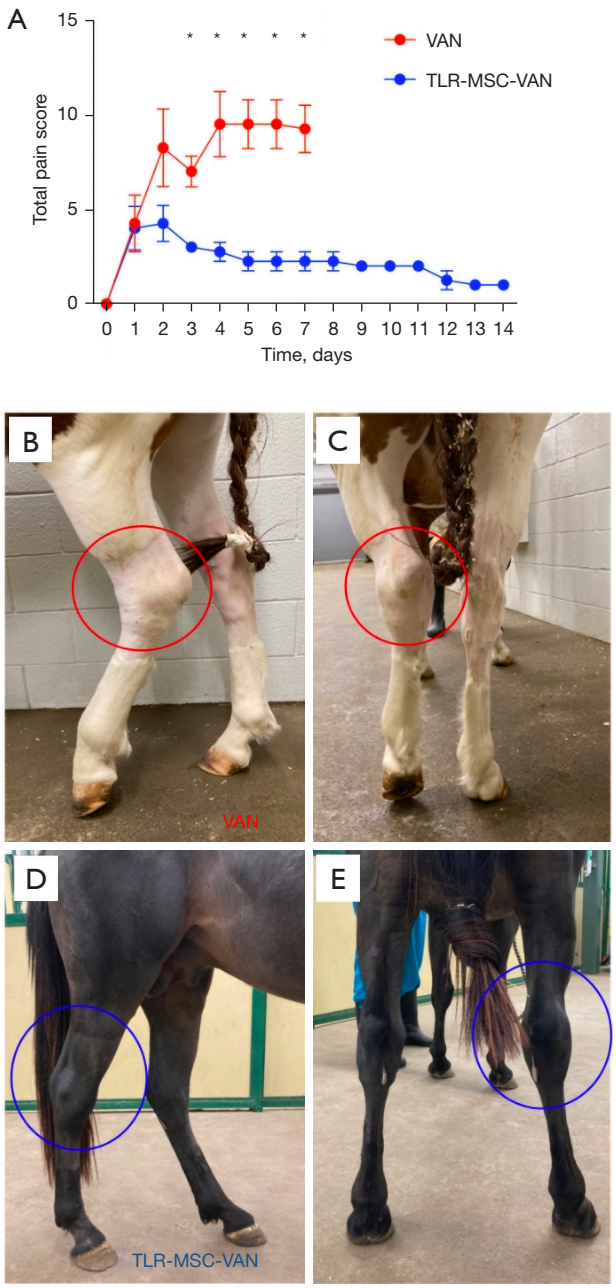

Figure 2 Pain scoring. (A) Overall pain scores were determined by grading a total of five parameters (physical examination including temperature, pulse rate, and respiratory rate, lameness evaluation, distal limb edema, joint circumference, synovial heat) on a scale of 0 to 3 (0= normal, 3= marked) for a maximum score of 15. Representative images shown for control (B,C) and treated (D,E) horses at end-term (day 7 or 14, respectively). *, significance was assessed at P<0.05. MSC, mesenchymal stromal cells; VAN, vancomycin.

a nearly 100% reduction in counts was seen in TLR-MSC-VAN, *vs.* 16% increase from d1 values in VAN. These findings indicated that TLR-MSC were effective in reducing bacterial survival, consistent with previous reports of the bactericidal activity of activated MSC (11,18).

SF responses to activated MSC therapy

We next addressed the question of how activated MSC injection affected cellular and cytokine responses in SF. (*Figure 6*). Serum amyloid A in SF was lower in TLR-MSC-VAN *vs.* VAN horses at end-term (0±0 *vs.* 2,094.0±601.6, P=0.01). Lactate was lower in TLR-MSC-VAN *vs.* VAN horses at d7 (5.4±0.2 *vs.* 15.0±0.3, P<0.0001). Total cell counts in SF of TLR-MSC-VAN horses were not different (P=0.09) compared to VAN-treated at d7. Total protein (P=0.08) and glucose concentrations were elevated (P=0.09) in the TLR-MSC-VAN group but did not reach statistical significance. When converted to absolute values, there were no detected differences in relative proportion of neutrophils, large or small mononuclear cells, eosinophils, or basophils. There were no detected differences in subjective glycosaminoglycan content or presence of red blood cells. SF IL-6 and IL-18 concentrations were significantly reduced in TLR-MSC-VAN *vs.* VAN groups (IL-6 across time points, 259.7±225.6 *vs.* 826.3±567.0, P=0.02; d4 313.0±119.2 *vs.* 1,328.2±208.9, P=0.03; IL-18 across time points 11.1±0.5 *vs.* 13.3±3.8, P=0.02) (*Figure 6*). Taken together, these findings are consistent with an overall reduction in IA inflammation following TLR-MSC-VAN administration.

Impact of activated MSC therapy on joint gross and microscopic pathology

We next addressed the question of whether cellular therapy altered the impact of infection on joint tissues, demonstrating lower overall macroscopic scores in TLR-MSC-VAN horses, accounting for synovial proliferation, subcutaneous edema, vascularity, and cartilage erosion (P=0.0003), results of which are illustrated in *Figure 7*. Joint inflammation, based on degree of neutrophilic inflammation, was reduced in TLR-MSC-VAN horses in the dorsolateral synovial quadrant (P=0.002). These findings indicate that early treatment with TLR-MSC can reduce overall joint pathology, which could be a combination of

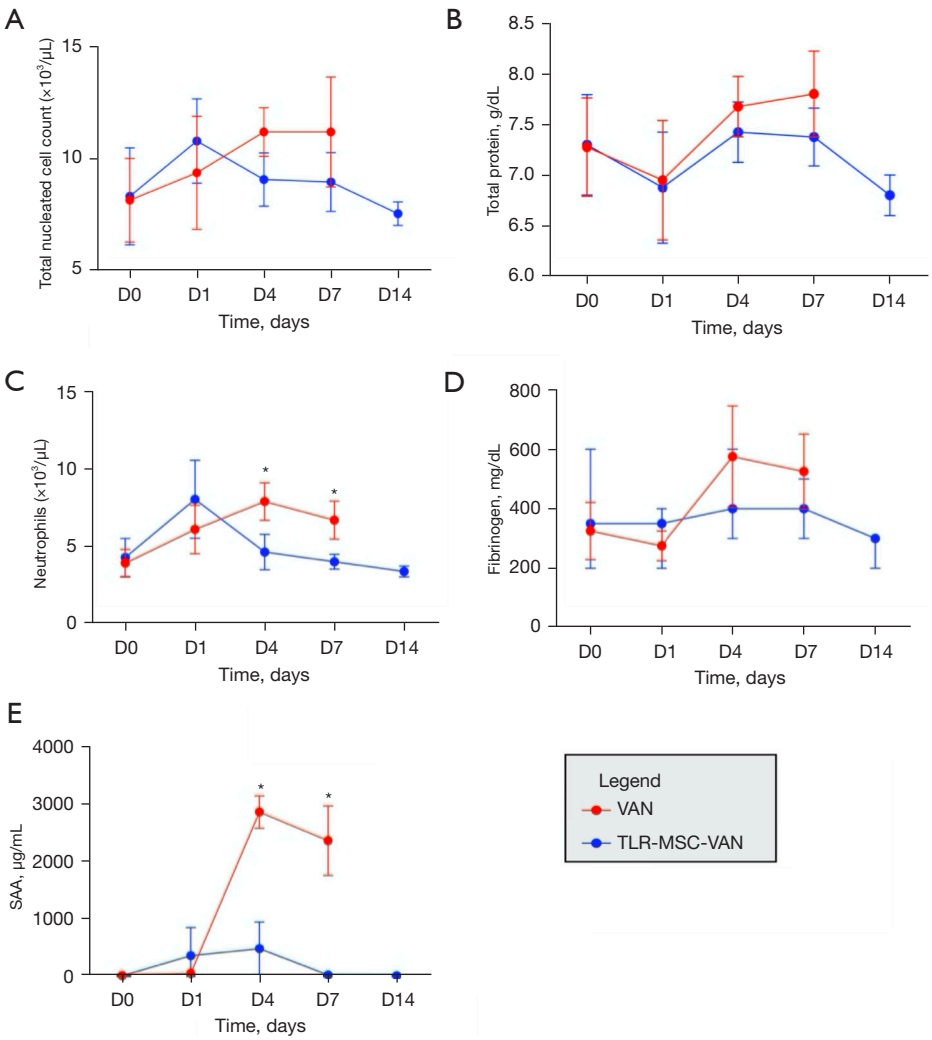

Figure 3 Systemic clinicopathologic parameters and biomarkers of inflammation. (A-D) Blood samples were collected on days 0, 1, 4, 7, and 14 in EDTA-containing tubes for complete blood count and leukocyte differential. (E) Quantification of SAA in plasma was performed using a handheld SAA test reader (StableLab, Epona Biotech Limited, Sligo, Ireland) according to manufacturer's instructions. *, significance was assessed at P<0.05. SAA, serum amyloid A; MSC, mesenchymal stromal cells; VAN, vancomycin.

direct and indirect effects mediated by the rapid reduction in bacterial burden.

Discussion

This study investigated the immunomodulatory and antimicrobial effects of intra-articular administration of TLR-3 activated MSC combined with antibiotics to treat multidrug resistant MRSA septic arthritis in an equine model. Addition of activated TLR-MSC to intra-articular VAN administration yielded improvement in clinical parameters and reduced biomarkers of inflammation and bacterial bioburden in SF of infected horses, compared to animals treated with VAN alone. The efficacy of the anti-infective cellular therapy approach in this large animal model suggests that a similar approach might be applied as a novel therapeutic strategy to treat multidrug resistant localized orthopedic infections.

S. aureus grows in 'free-floating biofilm aggregates' in SF, which have been shown to persist despite high concentrations of antimicrobials (25,44-47). Historically, there has been difficulty in isolating and culturing bacteria from SF of patients with infectious arthritis (48-50). Quantitative culture techniques described here were

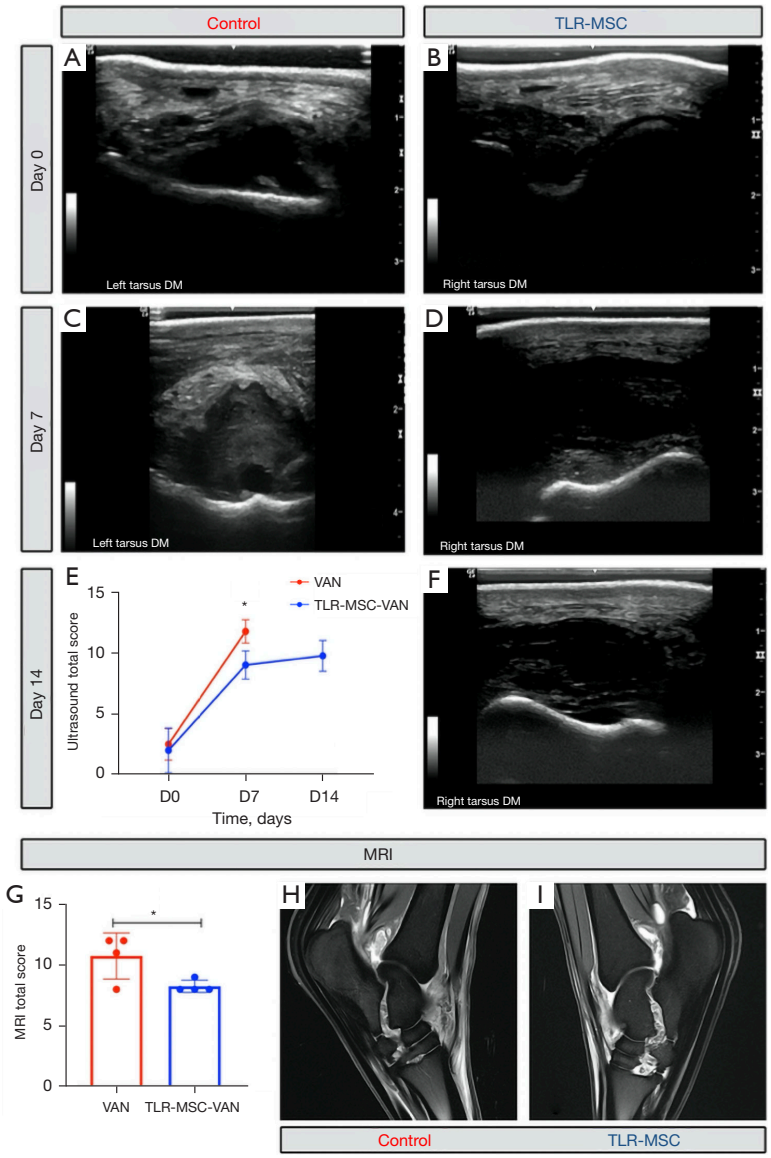

Figure 4 Imaging Scoring. Ultrasound images of VAN *vs.* TLR-MSC-VAN treated tarsi were obtained at days 0, 7, and 14 (treated horses only). Images were scored for degree of distention, degree of synovial thickening, degree of fibrinous loculation, and degree of vascularity as visualized with power Doppler were scored on a scale of 0 to 3 (0= normal, 3= markedly abnormal). Character of synovial effusion and presence of hyperechoic foci were scored on a scale of 0 or 1 (0= absent/anechoic, 1= present/echogenic). Representative images are shown for a horse treated with TLR-MSC-VAN and VAN at (B) baseline, (D) day 7, and (F) day 14, as well as a control horse treated with VAN alone at (A) baseline, (C) day 7. (E) Ultrasound scores were significantly improved in TLR-MSC-VAN *vs.* VAN horses on day 7 (P=0.03). MRI of the injected and control tarsi was performed immediately postmortem at end-term. MRI images were graded for degree of synovial distension, degree of synovial thickening, degree of fibrinous loculation on a scale of 0 to 3 (0= normal, 1= mild, 2= moderate, 3= markedly abnormal), boney proliferation at the joint capsule, subchondral bone lysis, subchondral bone sclerosis, osteophyte formation on a scale of 0 to 4 (0= none, 1= mild, 2= mild to moderate, 3= moderate, 4= severe), bone fluid on a scale of 0 to 4 (0= none, 1= mild, 2= mild to moderate, 3= moderate, 4= severe), and vascular pattern on a scale of 0 to 4 (0= none, 1= mild, 2= mild to moderate, 3= moderate, 4= severe). All imaging was evaluated by a board-certified veterinary radiologist (NW) unaware of treatment administered. (G) MRI scores were significantly lower (i.e., less severely abnormal) in TLR-MSC treated *vs.* control horses (P=0.08), when normalized to contralateral limb scores. Representative images are shown at end-term for (H) VAN and (I) TLR-MSC-VAN treated horses. *, significance was assessed at P<0.01. MSC, mesenchymal stromal cells; VAN, vancomycin; DM, dorsomedial.

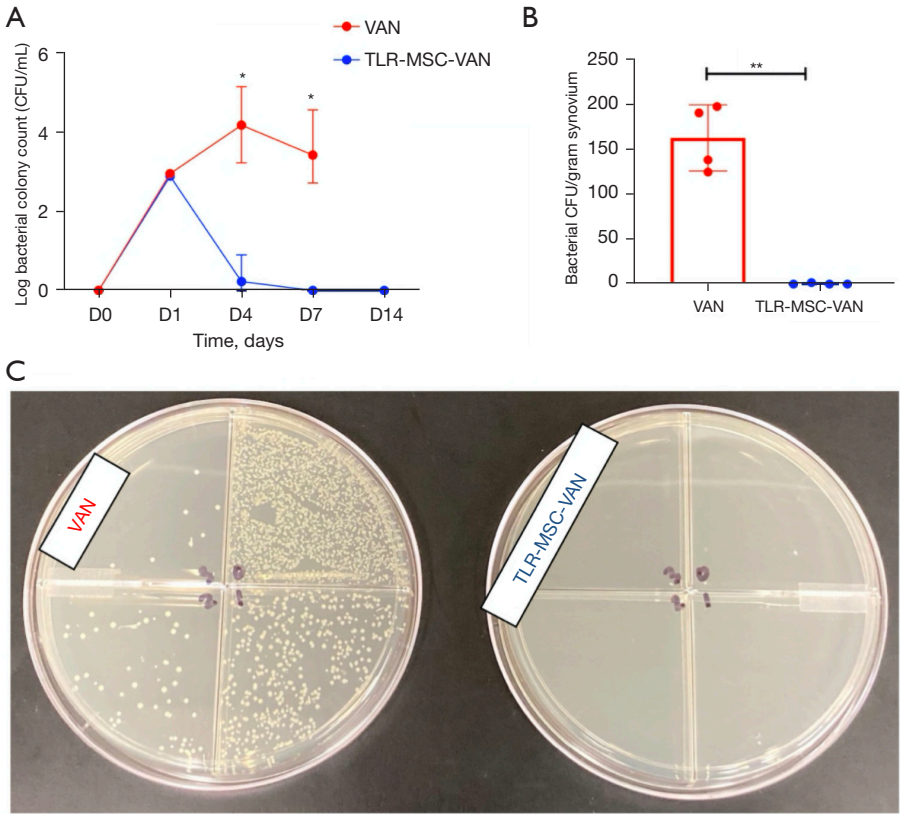

Figure 5 Quantitative bacterial culture of synovial fluid and synovium. Quantitative bacterial cultures were performed of (A) SF at days 0, 1, 4, 7, and 14 and of (B) synovium at end-term. Briefly, to generate quantitative cultures, synovial fluid aliquots were centrifuged at 8,000 g for 5 minutes and the supernatant was removed. The bacterial pellet was washed three times with PBS, resuspended in 1 mL PBS and incubated with 0.05 mg/mL hyaluronidase on a shaker at 120 rpm at 37 ℃ for 10 minutes to disperse any aggregated bacteria. Samples were then centrifuged again for 5 minutes and reconstituted in PBS for serial dilution. Synovium obtained aseptically at end-term was weighed and incubated with 1.5 mg/mL type 2 collagenase and 0.05 mg/mL hyaluronidase for one hour then pushed through a tissue strainer. Bacterial load was then determined using serial dilutions in PBS and plate CFU and reported as logarithm CFU/mL synovial fluid or per gram synovial tissue. (C) Representative images of quantitative culture quad-plates from VAN *vs.* TLR-MSC-VAN synovial fluid at day 7 shown. *, P<0.05; **, P<0.01. PBS, phosphate buffered saline; MSC, mesenchymal stromal cells; CFU, colony forming units; VAN, vancomycin.

based on novel experimental methods recently described and validated to accurately quantify *S. aureus* biofloat aggregates in SF as CFU per milliliter, utilizing enzymatic digestion to break up aggregates for effective and consistent determination of bacterial load (25,38). MSC have been previously described to express anti-biofilm activity thus resulting in eradication of infection due to floating biofilm aggregates. We believe this mechanism was demonstrated here, further validating anti-infective cellular therapy as a promising option to reduce bacterial load in joint infection (10,18). A recent study has shown that poly(I:C) preconditioning increases the abundance of extracellular vesicles (EV) proteins that have demonstrated antibiofilm activity (51). Thus, it is likely that poly(I:C) priming of MSC results in an amplification of antimicrobial effects. This upregulation of antimicrobial activity in several EV proteins critically contribute to the coagulation and complement cascades and affect modulation of innate immunity and the acute phase response. The complement system is critical for homeostasis, immunosurveillance and antimicrobial killing. Activation of the complement cascade yields in microbial killing through large pore-forming complexes resulting in rapid clearance of pathogens by immune cells. Given our clinical findings of resolving infection in the TLR-MSC-VAN treated horses, poly(I:C) priming is thought to regulate the immune system by activating the complement pathway,

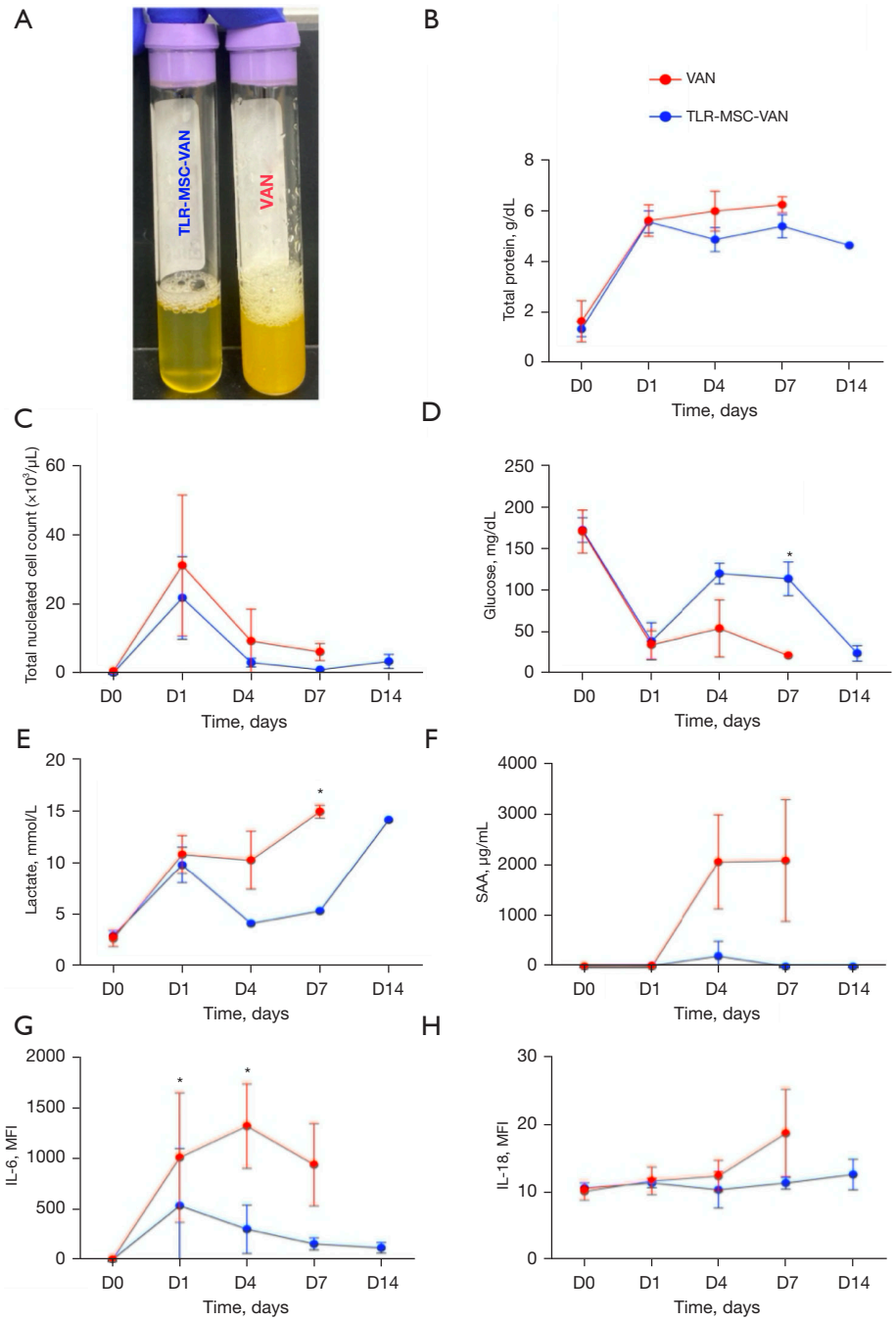

Figure 6 Evaluation of clinicopathologic parameters and biomarkers of inflammation in synovial fluid. SF samples (4 mL) were aspirated from the infected tibiotarsal joint at baseline (day 0) and at days 1, 4, 7, and 14. (A) Representative macroscopic images of synovial fluid obtained at day 4 from TLR-MSC-VAN *vs.* VAN horses. SF samples were assessed for (B) refractometric total protein and (C) total nucleated cell count (Hematrue, Heska Corp, Loveland, CO, USA) (D) glucose by handheld reader (AlphaTrak 2 Blood Glucose Monitoring System, Zoetis, Lincoln, NE, USA), (E) lactate by handheld reader (Lactate Plus Portable Lactate Reader, Nova Biomedical, Waltham, MA, USA), and (F) SAA by handheld reader (StableLab, Epona Biotech Limited, Sligo, Ireland). Fluorescent bead-based multiplex assay (Milliplex MAP Equine Cytokine/Chemokine Magnetic Beads Multiplex Assay, Millipore Sigma, Burlington, MA, USA) was used to quantify concentrations of 23 analytes in SF, with significant differences in (G) IL-6 and (H) IL-18 between TLR-MSC-VAN *vs.* VAN horses, reported in MFI. *, significance was assessed at $P<0.05$. SF, synovial fluid; MSC, mesenchymal stromal cells; VAN, vancomycin; SAA, serum amyloid A; MFI, mean fluorescence intensity.

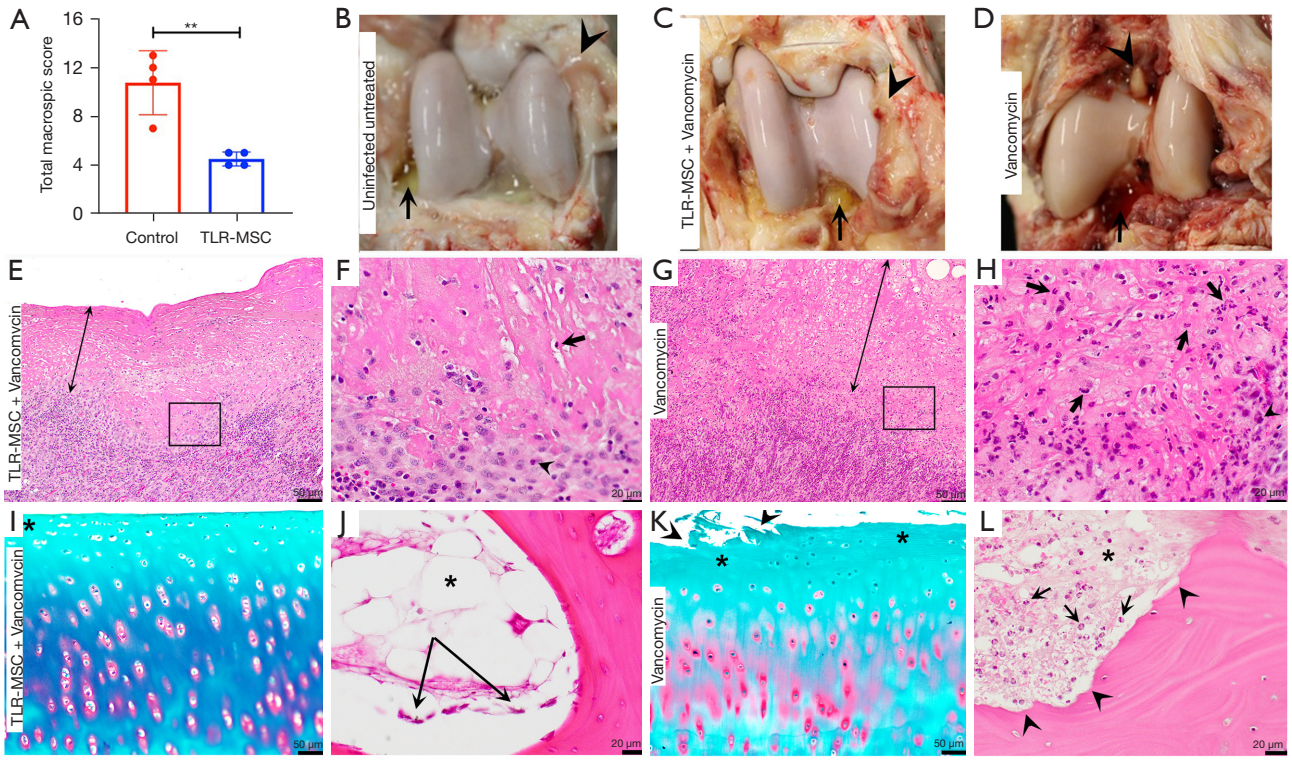

Figure 7 Pathology joint scoring at end-term. Assessment of macroscopic and microscopic observations was performed by consensus scoring of two-board certified equine surgeons using a modified macroscopic scoring system for septic arthritis, and a board-certified veterinary pathologist using a modified OARSI microscopic scoring system for synovial and osteochondral tissues, respectively. (A) Total macroscopic score reported as mean ± SD; macroscopic images of the tarsocrural joint from (B) uninfected, untreated limb, (C) infected joint treated with TLR-MSC-VAN, and (D) infected joint treated with VAN alone. Compared with the uninfected, untreated joint and the infected TLR-MSC-VAN joint, the articular cartilage, synovial membranes (arrowheads) and synovial fluid (arrows) of the infected joint treated with VAN alone show the most severe macroscopic lesions, including yellow discoloration of articular cartilage; synovial membrane hypertrophy with hyperemia, edema, hemorrhage, and fibrin exudate; and serosanguineous synovial effusion. Low (E,G) magnification, H&E stained histologic images of synovium from the dorsolateral compartment (scale bars =50 µm) from an infected joint treated with TLR-MSC-VAN (E,F) and an infected joint treated with VAN alone (G,H) show fibrin exudates (double-headed arrows) are more compacted and laminar within the TLR-MSC-VAN *vs.* VAN treated joint. At the synovial-exudate interface (framed regions), high magnification images (scale bars =20 µm) (F,H) show inflammatory cells within the synovium and exudate are predominantly mononuclear with rare neutrophils in TLR-MSC-VAN (F, arrows) compared to VAN treated joint where neutrophils within synovium and exudate comprise >50% of inflammatory cell infiltrates (H, arrows). Osteochondral sections from (I,J) infected joint treated with TLR-MSC-VAN and (K,L) VAN (I,K; scale bars =50 µm) show less severe surface fibrillation (arrowheads) and superficial chondrocyte loss (asterisks) in SafO stained sections of articular cartilage. In H&E stained sections of subchondral bone that immediately subtends the articular-epiphyseal complex (J,L; scale bars =20 µm) the endosteal interface in TLR-MSC-VAN treated joint (J) is smooth and lined by single rows of osteoblasts (arrows) with well-defined medullary adipocytes (asterisk) compared to VAN treated joint (L) where the endosteal margin is scalloped from osteoclast resorption lacunae (arrowheads) and the medullary adipocytes are effaced by eosinophilic fluid (asterisks) containing numerous viable and necrotic neutrophils (arrows). **, P<0.01. MSC, mesenchymal stromal cells; VAN, vancomycin.

regulating macrophage activation, reducing neutrophil adhesion, and enhancing phagocytosis.

The results of our study further support immunomodulation as a key mechanism of action for the antibacterial activity seen with TLR-MSC-VAN treatment. Treated horses displayed lower concentrations of IL-18, IL-6, and SAA. Harman *et al.* reported spontaneous production of AMPs by animal and human MSC, and

AMPs secreted by equine MSC inhibit the growth of bacteria commonly found in skin wounds (4). Johnson *et al.* explored the effects of MSC activation on the induction of bactericidal activity and observed that TLR-MSC treatment generates antibacterial activity in a mouse model (18). They further noted induction of neutrophil extracellular trap (NET) formation and increased neutrophil phagocytosis. These findings suggest that activation of MSC with TLR-3 ligands is thought to enhance production of immunomodulatory factors released by MSC augmenting the host innate immune responses to bacterial infections. Krasnodembskaya *et al.* proposed that the main mechanism of action from some of these cationic AMPs such as LL-37, expressed by immune cells via TLR stimulation, is by directly disrupting the integrity of the microbial membrane and by triggering the release of proinflammatory cytokines which in turn recruit immune cells (2). Compromised cell wall integrity in turn results in improved VAN penetration, increasing the ability for VAN to inhibit target sites during cell wall synthesis amplifying bacterial killing. In this study, reduction in joint inflammatory biomarkers could have been driven by direct reduction of bacterial bioburden or indirect interaction of MSC with the innate immune system resulting in immunomodulation. However, this study was not designed to distinguish these two possible mechanisms of action and the observed anti-inflammatory effect may have been mediated by a combination of both processes.

S. aureus use the host's coagulation system to accumulate fibrinous exudate and build fibrin-based biofloats (52-55). The decreased macroscopic scores in the MSC treated horses were primarily driven by a decrease in fibrinous synovial proliferation accumulation and subcutaneous thickening and may have been mitigated by decreased bacterial burden and associated fibrin deposition. No significant differences were noted for histological scoring overall or between each of four quadrants in treated *vs.* control horses, with the exception of neutrophil inflammation in the dorsolateral quadrant, which may be attributed to the relatively short time period between intra-articular bacterial inoculation and end-term. Further histologic differences pertaining to resolution of inflammatory changes and neutrophil infiltrates may have been seen if it had been possible for horses to continue on study longer, but this was not considered ethical.

Lack of consistency in cellular products and quality is a current challenge in effective implementation of cell-based therapies in clinical trials (56). The use of a pooled product from multiple donors was implemented in this study in an attempt to overcome variability in antimicrobial potency observed between donors *in vitro* (10). Major histocompatibility classes were determined for horses in this study, with two of four MSC recipients being partially matched and two being completely mismatched to the donor haplotypes. Further investigation of the effect of partial or full MHC incompatibility between donor and recipient horses on antibacterial efficacy with allogeneic MSC therapy is warranted. This may allow determination of whether matching MHC haplotype results in prolonged cell duration in the synovial space and therefore potentially enhanced antimicrobial effect. Screening of potential MSC donors for viral diseases transmitted through biological therapies would be indicated prior to clinical application and was not performed here due to the nature of experimental design and short study duration (57,58).

There are several limitations of this study, notably small sample size and relatively short survival time following inoculation. Further evaluation of treated horses beyond 14 days would have allowed for evaluation of recurrence of clinical signs of bacterial synovitis. The addition of control groups receiving non-activated MSC therapy for comparison and activated cells alone would increase overall rigor of our findings. However, number of horses evaluated (n=8) was sufficient to detect significant differences in multiple outcome parameters assessed (59). As the preselected level of significance was reached for many of the evaluated parameters, increasing the number of subjects would likely further decrease the P values and confirm the significance. The study design, using activated MSC combined with antimicrobial therapy, was based on previous data obtained by our group *in vitro* and in a mouse model of implant infection, demonstrating optimal antibacterial effect with TLR activation of MSC in combination with antibiotic therapy (10,11,18). Furthermore, duration of cell survival via tracking was not assessed in this study; however, previous work has demonstrated that intra-articularly injected MSC remain within joint tissues for one month following injection (60). Selection of gentamicin for administration in conjunction with MSC potentially represents a point for discussion due to its bacteriostatic *vs.* bactericidal nature; however, gentamicin was selected over other options for systemic use in horses (e.g., cephalosporins) based on the proposed bacterial isolate's sensitivity to this drug, its inexpensive cost, and appropriateness for use in veterinary species compared to alternatives considered reserved for use in human patients. In addition, the prolonged duration of administration of systemic antibiotics in the TLR-MSC-

VAN treated group represents a potential limitation in study design which is acknowledged; however, humane euthanasia of control VAN-treated horses was considered ethically necessary based on preliminary data from pilot horses and initial pain scoring and therefore these horses reached end-term at the earlier time point compared to TLR-MSC-VAN horses (d7 *vs.* d14). The concurrent nonsteroidal anti-inflammatory drugs (NSAIDs) throughout study duration was required to treat potential pain associated with intra-articular bacterial inoculation by the Institutional Animal Care and Use Committee, although admittedly the effect of NSAIDs on the immunomodulatory properties of injected MSC is unknown. However, the administration of NSAIDs would mimic the clinical scenario in which patients would be treated for septic arthritis and furthermore the use of NSAIDs as an adjunctive therapy was consistent across both treatment groups in dose, duration and frequency. Finally, future studies will build on those described to include investigation of cell delivery techniques including scaffolds to improve cell engraftment and microparticle release devices which may prolong the antibacterial effect observed compared to injection of single cell suspensions.

Conclusions

In summary, TLR-3 activated equine MSC therapy in combination with antibiotics reduced bacterial bioburden and improved clinical outcomes in treatment of antibiotic-resistant joint infections in a clinically relevant large animal model. *In vitro* TLR-3 activation of MSC prior to injection is a relatively simple method to enhance antimicrobial properties of MSC towards improved infection control. This anti-infective cellular technology offers an additional therapeutic strategy to augment current clinical practice when treating multidrug resistant infections.

Acknowledgments

The StableLab serum amyloid A testing material was kindly provided by Zoetis. The authors also gratefully acknowledge the assistance of Jen Daniels, Ryan Shelton, Natalie Lombard, Secorra Denny, Blaine Larson, Sherry Johnson and other staff members of the Orthopaedic Research Center for their assistance in data collection and kind care of university-owned research horses. The authors also thank Josh Daniels for his assistance with study design and development of bacteriological culture methods, Ann Hess for her assistance with statistical analysis, and Dean Hendrickson and Jason Stoneback for their contributions to and discussion of study design. Finally, the authors thank C. Wayne McIlwraith for his observations on the study horses.
Funding: This work was supported by the Grayson Jockey Club Research Foundation, ACVS Zoetis Dual Training Grant, NIH/NCATS CTSA 5TL1TR002533-02, NIH 5T32OD010437-19, Verdad Foundation, Charles Shipley Family Foundation and Carolyn Quan and Porter Bennett.

Footnote

Reporting Checklist: The authors have completed the ARRIVE reporting checklist. Available at https://atm.amegroups.com/article/view/10.21037/atm-22-1746/rc

Data Sharing Statement: Available at https://atm.amegroups.com/article/view/10.21037/atm-22-1746/dss

Peer Review File: Available at https://atm.amegroups.com/article/view/10.21037/atm-22-1746/prf

Conflicts of Interest: All authors have completed the ICMJE uniform disclosure form (available at https://atm.amegroups.com/article/view/10.21037/atm-22-1746/coif). LMP, LC, SD, and LRG declare that a patent application has been filed covering the antimicrobial cellular therapy technology described here. LMP reports that support for this work was provided by the Grayson Jockey Club Research Foundation, ACVS Zoetis Dual Training Grant, NIH/NCATS CTSA 5TL1TR002533-02, NIH 5T32ODO010437-19, Verdad Foundation, Charles Shipley Family Foundation and Carolyn Quan and Porter Bennett. The StableLab serum amyloid A testing material was kindly provided by Zoetis. LMP reports that she holds stock options in eQCell Inc. SD reports that he holds stock options in eQCell Inc. LRG reports that she holds stock options in eQCell and Advanced Regenerative Therapies. The other authors have no conflicts of interest to declare.

Ethical Statement: The authors are accountable for all aspects of the work in ensuring that questions related to the accuracy or integrity of any part of the work are appropriately investigated and resolved. This study was approved by the Institutional Animal Care and Use Committee at Colorado State University (No. CSU IACUC #977) and conducted according to the national guidelines under which the institution operates, and NIH Guidelines for the Care and Use of Laboratory Animals (8th edition).

References

1. Mezey É, Nemeth K. Mesenchymal stem cells and infectious diseases: Smarter than drugs. Immunol Lett 2015;168:208-14.
2. Krasnodembskaya A, Song Y, Fang X, et al. Antibacterial effect of human mesenchymal stem cells is mediated in part from secretion of the antimicrobial peptide LL-37. Stem Cells 2010;28:2229-38.
3. Krasnodembskaya A, Samarani G, Song Y, et al. Human mesenchymal stem cells reduce mortality and bacteremia in gram-negative sepsis in mice in part by enhancing the phagocytic activity of blood monocytes. Am J Physiol Lung Cell Mol Physiol 2012;302:L1003-13.
4. Harman RM, Yang S, He MK, et al. Antimicrobial peptides secreted by equine mesenchymal stromal cells inhibit the growth of bacteria commonly found in skin wounds. Stem Cell Res Ther 2017;8:157.
5. Cortés-Araya Y, Amilon K, Rink BE, et al. Comparison of Antibacterial and Immunological Properties of Mesenchymal Stem/Stromal Cells from Equine Bone Marrow, Endometrium, and Adipose Tissue. Stem Cells Dev 2018;27:1518-25.
6. Ghannam S, Bouffi C, Djouad F, et al. Immunosuppression by mesenchymal stem cells: mechanisms and clinical applications. Stem Cell Res Ther 2010;1:2.
7. Kwon DG, Kim MK, Jeon YS, et al. State of the Art: The Immunomodulatory Role of MSCs for Osteoarthritis. Int J Mol Sci 2022;23:1618.
8. Németh K, Leelahavanichkul A, Yuen PS, et al. Bone marrow stromal cells attenuate sepsis via prostaglandin E(2)-dependent reprogramming of host macrophages to increase their interleukin-10 production. Nat Med 2009;15:42-9.
9. de Witte SFH, Luk F, Sierra Parraga JM, et al. Immunomodulation By Therapeutic Mesenchymal Stromal Cells (MSC) Is Triggered Through Phagocytosis of MSC By Monocytic Cells. Stem Cells 2018;36:602-15.
10. Pezzanite LM, Chow L, Johnson V, et al. Toll-like receptor activation of equine mesenchymal stromal cells to enhance antibacterial activity and immunomodulatory cytokine secretion. Vet Surg 2021;50:858-71.
11. Chow L, Johnson V, Impastato R, et al. Antibacterial activity of human mesenchymal stem cells mediated directly by constitutively secreted factors and indirectly by activation of innate immune effector cells. Stem Cells Transl Med 2020;9:235-49.
12. Le Blanc K, Mougiakakos D. Multipotent mesenchymal stromal cells and the innate immune system. Nat Rev Immunol 2012;12:383-96.
13. Mei SH, Haitsma JJ, Dos Santos CC, et al. Mesenchymal stem cells reduce inflammation while enhancing bacterial clearance and improving survival in sepsis. Am J Respir Crit Care Med 2010;182:1047-57.
14. Monneret G. Mesenchymal stem cells: another anti-inflammatory treatment for sepsis? Nat Med 2009;15:601-2; author reply 602.
15. Kim J, Hematti P. Mesenchymal stem cell-educated macrophages: a novel type of alternatively activated macrophages. Exp Hematol 2009;37:1445-53.
16. Lee JW, Gupta N, Serikov V, et al. Potential application of mesenchymal stem cells in acute lung injury. Expert Opin Biol Ther 2009;9:1259-70.
17. Cruz FF, Weiss DJ, Rocco PR. Prospects and progress in cell therapy for acute respiratory distress syndrome. Expert Opin Biol Ther 2016;16:1353-60.
18. Johnson V, Webb T, Norman A, et al. Activated Mesenchymal Stem Cells Interact with Antibiotics and Host Innate Immune Responses to Control Chronic Bacterial Infections. Sci Rep 2017;7:9575.
19. Frisbie DD, Cross MW, McIlwraith CW. A comparative study of articular cartilage thickness in the stifle of animal species used in human pre-clinical studies compared to articular cartilage thickness in the human knee. Vet Comp Orthop Traumatol 2006;19:142-6.
20. McIlwraith CW, Fortier LA, Frisbie DD, et al. Equine Models of Articular Cartilage Repair. Cartilage 2011;2:317-26.
21. McIlwraith CW, Frisbie DD, Kawcak CE. The horse as a model of naturally occurring osteoarthritis. Bone Joint Res 2012;1:297-309.
22. Chu CR, Szczodry M, Bruno S. Animal models for cartilage regeneration and repair. Tissue Eng Part B Rev 2010;16:105-15.
23. Reesink HL, Watts AE, Mohammed HO, et al. Lubricin/proteoglycan 4 increases in both experimental and

naturally occurring equine osteoarthritis. Osteoarthritis Cartilage 2017;25:128-37.
24. Frisbie DD, Kawcak CE, Trotter GW, et al. Effects of triamcinolone acetonide on an in vivo equine osteochondral fragment exercise model. Equine Vet J 1997;29:349-59.
25. Gilbertie JM, Schnabel LV, Hickok NJ, et al. Equine or porcine synovial fluid as a novel ex vivo model for the study of bacterial free-floating biofilms that form in human joint infections. PLoS One 2019;14:e0221012.
26. Wright IM, Smith MR, Humphrey DJ, et al. Endoscopic surgery in the treatment of contaminated and infected synovial cavities. Equine Vet J 2003;35:613-9.
27. Ludwig EK, van Harreveld PD. Equine Wounds over Synovial Structures. Vet Clin North Am Equine Pract 2018;34:575-90.
28. Glass K, Watts AE. Septic Arthritis, Physitis, and Osteomyelitis in Foals. Vet Clin North Am Equine Pract 2017;33:299-314.
29. Taylor S. A review of equine sepsis. Equine Vet Educ 2015;27:99-109.
30. Lugo J, Gaughan EM. Septic arthritis, tenosynovitis, and infections of hoof structures. Vet Clin North Am Equine Pract 2006;22:363-88, viii.
31. Nelson BB, Mäkelä JTA, Lawson TB, et al. Evaluation of equine articular cartilage degeneration after mechanical impact injury using cationic contrast-enhanced computed tomography. Osteoarthritis Cartilage 2019;27:1219-28.
32. Gilbertie JM, Schaer TP, Engiles JB, et al. A Platelet-Rich Plasma-Derived Biologic Clears Staphylococcus aureus Biofilms While Mitigating Cartilage Degeneration and Joint Inflammation in a Clinically Relevant Large Animal Infectious Arthritis Model. Front Cell Infect Microbiol 2022;12:895022.
33. Schnabel LV, Fortier LA, McIlwraith CW, et al. Therapeutic use of stem cells in horses: which type, how, and when? Vet J 2013;197:570-7.
34. Holmes CM, Violette N, Miller D, et al. MHC haplotype diversity in Icelandic horses determined by polymorphic microsatellites. Genes Immun 2019;20:660-70.
35. Radcliffe CH, Flaminio MJ, Fortier LA. Temporal analysis of equine bone marrow aspirate during establishment of putative mesenchymal progenitor cell populations. Stem Cells Dev 2010;19:269-82.
36. Schnabel LV, Pezzanite LM, Antczak DF, et al. Equine bone marrow-derived mesenchymal stromal cells are heterogeneous in MHC class II expression and capable of inciting an immune response in vitro. Stem Cell Res Ther 2014;5:13.
37. Esteves CL, Sheldrake TA, Mesquita SP, et al. Isolation and characterization of equine native MSC populations. Stem Cell Res Ther 2017;8:80.
38. Dominici M, Le Blanc K, Mueller I, et al. Minimal criteria for defining multipotent mesenchymal stromal cells. The International Society for Cellular Therapy position statement. Cytotherapy 2006;8:315-7.
39. Rasband WS. Image J, U.S. (1997–2018). Bethesda, Maryland, USA: National Institutes of Health; 2018. Available online: https://imagej.nih.gov/ij/
40. Gilbertie JM, Schaer TP, Schubert AG, et al. Platelet-rich plasma lysate displays antibiofilm properties and restores antimicrobial activity against synovial fluid biofilms in vitro. J Orthop Res 2020;38:1365-74.
41. McIlwraith CW, Frisbie DD, Kawcak CE, et al. The OARSI histopathology initiative - recommendations for histological assessments of osteoarthritis in the horse. Osteoarthritis Cartilage 2010;18 Suppl 3:S93-105.
42. Kassambara A. rstatix: Pipe-Friendly Framework for Basic Statistical Tests (R package version 0.7.0) 2021. [Computer software].
43. R Core Team. R: A language and environment for statistical computing. 2021. R Foundation for Statistical Computing, Vienna, Austria.
44. Weston VC, Jones AC, Bradbury N, et al. Clinical features and outcome of septic arthritis in a single UK Health District 1982-1991. Ann Rheum Dis 1999;58:214-9.
45. Dastgheyb S, Parvizi J, Shapiro IM, et al. Effect of biofilms on recalcitrance of staphylococcal joint infection to antibiotic treatment. J Infect Dis 2015;211:641-50.
46. Dastgheyb SS, Hammoud S, Ketonis C, et al. Staphylococcal persistence due to biofilm formation in synovial fluid containing prophylactic cefazolin. Antimicrob Agents Chemother 2015;59:2122-8.
47. Perez K, Patel R. Biofilm-like aggregation of Staphylococcus epidermidis in synovial fluid. J Infect Dis 2015;212:335-6.
48. Gilbertie JM, Schnabel LV, Stefanovski D, et al. Gram-negative multi-drug resistant bacteria influence survival to discharge for horses with septic synovial structures: 206 Cases (2010-2015). Vet Microbiol 2018;226:64-73.
49. Taylor AH, Mair TS, Smith LJ, et al. Bacterial culture of septic synovial structures of horses: does a positive bacterial culture influence prognosis? Equine Vet J 2010;42:213-8.
50. Gallo J, Kolar M, Dendis M, et al. Culture and PCR analysis of joint fluid in the diagnosis of prosthetic joint infection. New Microbiol 2008;31:97-104.

51. Pierce LM, Kurata WE. Priming With Toll-Like Receptor 3 Agonist Poly(I:C) Enhances Content of Innate Immune Defense Proteins but Not MicroRNAs in Human Mesenchymal Stem Cell-Derived Extracellular Vesicles. Front Cell Dev Biol 2021;9:676356.
52. Crosby HA, Kwiecinski J, Horswill AR. Staphylococcus aureus Aggregation and Coagulation Mechanisms, and Their Function in Host-Pathogen Interactions. Adv Appl Microbiol 2016;96:1-41.
53. Loof TG, Goldmann O, Naudin C, et al. Staphylococcus aureus-induced clotting of plasma is an immune evasion mechanism for persistence within the fibrin network. Microbiology (Reading) 2015;161:621-7.
54. Speziale P, Pietrocola G, Foster TJ, et al. Protein-based biofilm matrices in Staphylococci. Front Cell Infect Microbiol 2014;4:171.
55. Zapotoczna M, McCarthy H, Rudkin JK, et al. An Essential Role for Coagulase in Staphylococcus aureus Biofilm Development Reveals New Therapeutic Possibilities for Device-Related Infections. J Infect Dis 2015;212:1883-93.
56. Trivedi A, Miyazawa B, Gibb S, et al. Bone marrow donor selection and characterization of MSCs is critical for pre-clinical and clinical cell dose production. J Transl Med 2019;17:128.
57. Tomlinson JE, Jager M, Struzyna A, et al. Tropism, pathology, and transmission of equine parvovirus-hepatitis. Emerg Microbes Infect 2020;9:651-63.
58. Tomlinson JE, Kapoor A, Kumar A, et al. Viral testing of 18 consecutive cases of equine serum hepatitis: A prospective study (2014-2018). J Vet Intern Med 2019;33:251-7.
59. Gorzalczany SB, Rodriguez Basso AG. Strategies to apply 3Rs in preclinical testing. Pharmacol Res Perspect 2021;9:e00863.
60. Satué M, Schüler C, Ginner N, et al. Intra-articularly injected mesenchymal stem cells promote cartilage regeneration, but do not permanently engraft in distant organs. Sci Rep 2019;9:10153.

Cite this article as: Pezzanite LM, Chow L, Phillips J, Griffenhagen GM, Moore AR, Schaer TP, Engiles JB, Werpy N, Gilbertie J, Schnabel LV, Antczak D, Miller D, Dow S, Goodrich LR. TLR-activated mesenchymal stromal cell therapy and antibiotics to treat multi-drug resistant *Staphylococcal* septic arthritis in an equine model. Ann Transl Med 2022;10(21):1157. doi: 10.21037/atm-22-1746

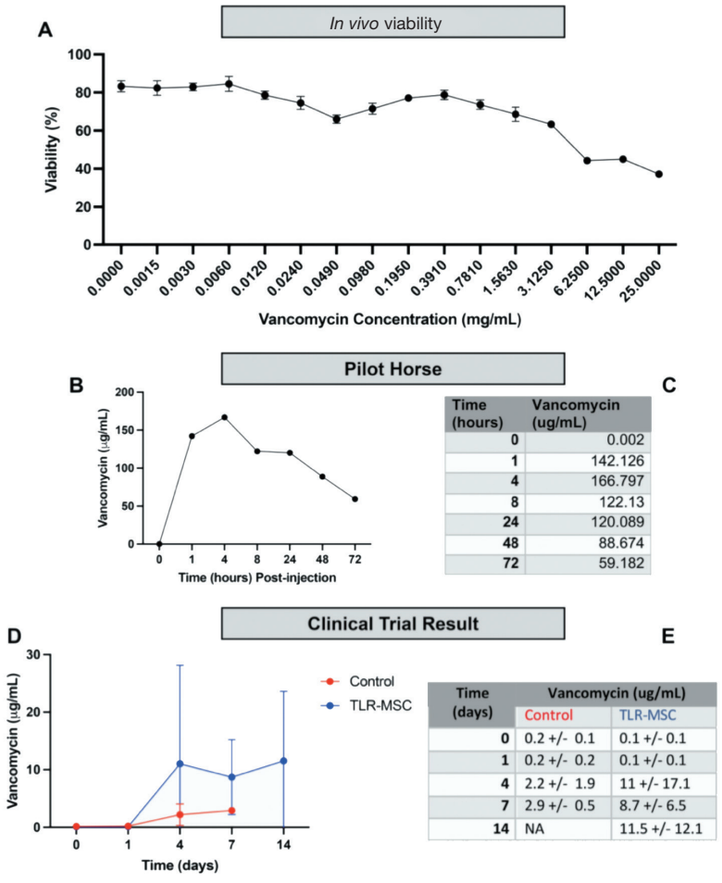

Figure S1 Pilot data towards determination of vancomycin dose and concentrations in synovial fluid in treated *vs.* control horses. (A) Effect of VAN on viability of equine bone marrow-derived mesenchymal stromal cells in monolayer culture. Cell viability (mean±SD) was assessed in MSC from each of three donor horses, each in triplicate, using trypan blue dye exclusion staining to determine percentage of live cells following antibiotic exposure for 24 hours. X-axis represents antibiotic concentration; y-axis represents percentage of live cells. Dose response for each concentration was normalized to control, and the data transformed to 'normalized dose response *vs.* log10 (concentration)' at which point the half maximal inhibitory concentration (IC50) was estimated by nonlinear regression implemented in GraphPad Prism8 (GraphPad Software Prism8). (B) VAN (100 mg) was injected in the tibiotarsal joint of a 3-year-old Quarter Horse mare and synoviocenteses performed at baseline and 1, 4, 8, 24, 48, and 72 hours following injection to obtain synovial fluid samples (1 to 2 mL). VAN concentrations in synovial fluid were assessed via immunoassay (BioVision, Milpitas, CA, USA 95035)), and (C) remained above MIC for the targeted pathogen (1 µg/mL) at 72 hours following injection. (D) VAN levels in synovial fluid were determined and (E) remained above 1 µg/mL in both treatment and control horses at each of the time points following administration (days 4, 7, 14). VAN levels varied widely between individuals but were not significantly different overall between VAN or TLR-MSC-VAN treated horses at any time point.

https://dx.doi.org/10.21037/atm-22-1746

Table S1 Microsatellite haplotype data for MSC donor and treatment recipient horses.

Horse	Microsatellite haplotype	Intra-MHC Microsatellite Alleles											
		Class I				Class III		Class II					
		UMNJH-38	COR110	305-93	CZM002	ABGe9019	UMNe65	ABGe9030	EQMHC1	COR112	COR113	UM011	COR114
MSC Donor Horses													
A	ELA-A9a	156	217	0	247	307	255	215	190	264	272	169	255
	ELA-A5a	156	221	0	261	299	257	212	190	254	260	172	243
B	ELA-A5a	156	221	0	261	299	257	212	190	254	260	172	243
	ELA-A10a	156	221	0	259	312	261	207	190	237	264	180	243
C	ELA-A5a	156	221	0	261	299	257	212	190	254	260	172	243
	ELA-A3b	163	207	0	251	312	261	211	192	262	268	176	247
Treatment Recipient Horses													
Control													
A	Not phased	156	211	342	249	301	259	205	192	250	266	169	245
	Not phased	156	221	345	232	310	263	217	199	254	266	170	249
B	ELA-A5a	156	221	340	261	299	257	212	190	254	260	172	243
	Novel	161	211	341	255	314	259	219	190	262	270	184	245
C	Not phased	156	215	345	253	312	257	221	180	252	274	171	243
	Not phased	156	211	345	259	299	261	215	190	260	266	169	249
D	Novel	161	211	341	255	312	261	207	190	237	264	180	243
	ELA-A3b	163	207	343	251	312	261	211	192	262	268	176	247
Treatment (MSC Recipients)													
E	ELA-A3b	163	207	343	251	312	259	211	192	262	268	176	247
	Novel	156	215	345	251	312	259	221	180	252	274	171	243
F	COR-188	156	221	342	230	318	257	219	190	254	270	172	249
	Novel	156	219	347	230	316	263	215	190	237	268	176	247
G	Not Phased	156	207	340	230	314	257	215	190	262	260	172	243
	Not Phased	156	207	346	261	316	259	215	196	268	268	176	247
H	ELA-A2	156	211	343	249	301	259	209	192	262	268	174	234
	ELA-A5a	156	221	340	261	299	257	212	190	254	260	172	243

https://dx.doi.org/10.21037/atm-22-1746

Table S2 Histological scoring system for synovium tissues

Fibrin exudate (0-4)	Cellular infiltrate (neutrophils)	Vascularity	Intimal ulceration
0 = none	0 = none	0 = normal	0 = none
1 = occasional small scattered foci	1 = occasional small foci / infiltrates	1 = slight increase vessels in focal areas	1 = occasional small scattered foci
2 = confluent mats <25% total surface	2 = neutrophils 25% inflammatory infiltrate	2 = mild increase number and dilation throughout	2 = 25–50% total surface area
3 = mats 25 to 50% total surface	3 = neutrophils 25% to 50% infiltrates	3 = moderate increase number and dilation <50% section	3 = >50–75% total surface area
4 = mats >50% total surface	4 = neutrophils >50% infiltrates	4 = marked increase >50% of section	4 = >75% total surface area
Intimal hyperplasia	**Subintimal edema**	**Subintimal fibrosis/Granulation tissue**	
0 = none	0 = no edema	0 = normal	
1 = villi with 2 to 4 rows intimal cells	1 = slight edema detected in section	1 = slight increase in fibrosis within section	
2 = villi with 4 to 5 rows intimal cells over 25 to 50% section	2 = mild edema 25% of section	2 = mild increased fibrosis within 25% section	
3 = villi with 4 to 5 rows intimal cells >50% section	3 = moderate edema with 25–50% section	3 = moderate increased fibrosis within 25-50% section	
4 = villi with >5 rows intimal cells over 50% section	4 = marked edema >50% section	4 = marked increased fibrosis within >50% section	
5 = diffusely ulcerated intima			

Table S3 Histological scoring system for osteochondral tissues

Cartilage parameters				
Chondrocyte necrosis	Chondrones	Fibrillation/fissures	Focal cell loss	SafO stain uptake
0 = none	0 = none	0 = no fibrillation/fissures	0 = 0%	0 = 0%
1 = 1 necrotic cell near surface per 20× objective	1 = 2 chondrone nuclei (doublets)	1 = fibrillation/fissures restricted to surface, superficial zone	1 = 10–20% acellularity per 20× field	1 = <25%
2 = 1 to 2 necrotic cells	2 = 2 to 3 chondrone nuclei	2 = fissures extend to middle zone	2 = 20–30% acellularity	2 = 25–50%
3 = 2 to 3 necrotic cells	3 = 3 to 4 chondrone nuclei	3 = fissures extend to level of deep zone	3 = 40–50% acellularity	3 = 50–75%
4 = 3 to 4 necrotic cells	4 = >4 chondrone nuclei	4 = fissures extend to deep zone	4 = >50% acellularity per 20× field	4 = >75%
Bone parameters				
Osteochondral lesions	**Subchondral bone remodeling**	**Subchondral bone activation**	**Osteochondral splitting**	
0 = no visible changes in cartilage or bone	0 = no remodeling	0 = no remodeling	0 = no splitting	
1 = minor disruption of subchondral bone matrix <25% of condylar surface, no cartilage fibrillation	1-scalloped remodeling, no tidemarks crossed	1 = hyperemic/edematous osteonal spaces	1 = splitting involves tidemark and subchondral bone but simple linear defects	
	2 = remodeling crosses deep tidemarks, superficial tidemark intact	2 = OB activation	2 = fragments and debris within splits and connections between splits	
	3 = remodeling crosses tidemark front	3 = OCL activation/scalloped margins of osteons	3 = involve articular cartilage with displacement of fragments	
		4 = subchondral OCL and OB activation with inflammation		

https://dx.doi.org/10.21037/atm-22-1746